J. Mol. Biol. (1996) **258**, 6–13

JMB

COMMUNICATION

Alanine Substitutions in Calmodulin-binding Peptides Result in Unexpected Affinity Enhancement

Silvia Montigiani[1], Giovanni Neri[1], Paolo Neri[1] and Dario Neri[2]*

[1]*Dipartimento di Biologia Molecolare, Sezione di Immunochimica, Universita' di Siena, Centro Didattico loc. Le Scotte, 53100 Siena Italy*

[2]*Cambridge Centre for Protein Engineering MRC Centre, Hills Road Cambridge, CB2 2QH England*

**Corresponding author*

Calmodulin is a calcium-binding protein that regulates a wide range of enzymes. It is also one of the few examples of a small protein capable of binding to peptides with very high affinity, and is therefore an interesting candidate for biotechnological applications and a good model system for studying how proteins associate.

We have synthesized a complete series of peptides derived from the recognition sequence of skeletal muscle myosin light-chain kinase, corresponding to single-point amino acid mutations to alanine. These peptides bind to calmodulin with a biphasic kinetic: a fast association step followed by a slow intramolecular isomerisation. We have measured the isomerisation rate (k_{isom}) of these peptides for calmodulin by stopped-flow analysis, and their association and dissociation kinetic constants (k_{on} and k_{off}) by real-time interaction analysis using surface plasmon resonance detection. In addition, k_{off} constants were measured by competition experiments using a high-sensitivity luminescence analyser and native polyacrylamide gels.

We have observed that all the alanine-scanning peptides bound to calmodulin with better affinity than the wild-type. In one case, a Asn→Ala substitution resulted in a 1000-fold improvement in affinity, owing to a slower off-rate.

Our results indicate that naturally occurring calmodulin binders may have evolved to have high affinities, but far from the maximum. Our affinity data are in contrast with recently published predictions of interactions responsible for high-affinity calmodulin binding based on modelling and energy calculations.

Keywords: calmodulin; calmodulin binding peptides; kinetic association constants; kinetic dissociation constants; alanine scanning

Calmodulin is a small, well-conserved protein (148 residues) and with a key role in intracellular signal transduction, folding in the presence of calcium, and binding and activating enzymes (Lukas *et al*., 1988). Three-dimensional structures of calmodulin in complex with high-affinity peptidic substrates are available (Ikura *et al*., 1992; Meador *et al*., 1992, 1993). These peptides correspond to the calmodulin-binding regions of different protein kinases, whose general mechanism of activation by calmodulin is a matter of considerable biological interest. Furthermore, the high-affinity binding of calmodulin to both peptidic and non-peptidic substrates can be abolished by addition of calcium chelators, making this system an interesting candidate for biotechnological applications (Neri *et al*., 1995); for example, as a useful alternative to the avidin–biotin system (Bayer & Wilcheck, 1990).

Calmodulin–peptide complexes are convenient models for determining how proteins associate and dissociate, which is fundamental to molecular recognition and activation processes in biology. For example, O'Neil & DeGrado (1989) have studied this system to design peptides forming a putative amphiphilic helix and binding to calmodulin with subnanomolar dissociation constants (K_d). With the three-dimensional structures available (Ikura *et al*., 1992; Meador *et al*., 1992, 1993), it is now possible to extend this research further. We can now use the

Abbreviations used: sMLCK, skeletal myosin light chain kinase; TBS, Tris-buffered saline; TBSC, Tris-buffered saline + 50 μM $CaCl_2$; TEMED, *N*,*N*,*N*',*N*'-tetramethylethylenediamine.

0022–2836/96/160006–08 $18.00/0

calmodulin–ligand complex system to investigate how proteins recognise each other in a high-affinity interaction.

The NMR structure of the complex between calmodulin and a 26 amino acid peptide derived from rabbit skeletal myosin light chain kinase (sMLCK; Ikura *et al*., 1992) has shown that only the central 19-mer sequence RWKKNFIAVSAANR-FKKIS contacts calmodulin. We have therefore chosen the 23-mer peptide CAAA-RWKKNFI-AVSAANRFKKIS-CONH$_2$ (C-terminal amide) as a model for our study, the first cysteine residue serving for site-specific peptide functionalisation with thiol-specific reagents (such as iodoacetamido fluorescein or biotin derivatives) and the following three alanine residues as spacers. We have synthesised peptides 2 to 17 (Figure 1) corresponding to alanine mutations of all the non-alanine residues in the calmodulin recognition sequence. Figure 1 shows that all these peptides bind to calmodulin in native polyacrylamide gels (Neri *et al*., 1995), indicating that single alanine substitutions have no severely deleterious effects on calmodulin binding.

Török & Trentham (1994) have shown by stopped-flow analysis that smooth-muscle MLCK-derived peptides bind to calmodulin with a biphasic kinetic according to Scheme 1:

$$P + C \underset{k_{-1}}{\overset{k_{+1}}{\rightleftharpoons}} P - C \underset{k_{-2}}{\overset{k_{+2}}{\rightleftharpoons}} P - C^*$$

in which P is the peptide, C is calmodulin, P–C is the first complex formed upon association of P and C, which then undergoes a conformational isomerisation to P–C*.

Stopped-flow analysis of calmodulin binding to our skeletal MLCK-derived peptides confirms a biphasic binding kinetic (Figure 2(a)). The isomerisation constant ($k_{+2} + k_{-2}$) and association constant k_{+1}($\sim 10^{-1}$ s^{-1} and $\sim 10^{6}$ s^{-1} M^{-1}, respectively) for skeletal MLCK-derived peptides are lower than those of smooth-muscle MLCK-derived peptides ($\sim 10^{0}$ s^{-1} and 10^{8}–10^{9} s^{-1} M^{-1}, respectively; Török & Trentham, 1994), which required the site-specific calmodulin labelling with an environment-sensitive fluorescent probe and the use of low concentrations for accurate measurements.

For a kinetic and thermodynamic characterisation of the binding of our alanine scanning peptides to bovine brain calmodulin, we have therefore measured kinetic isomerisation, association and dissociation constants (k_{isom}, k_{on} and k_{off}), from which dissociation constants K_d can be derived.

According to the nomenclature of Scheme 1 and to Török & Trentham (1994):

$$k_{isom} = k_{+2} + k_{-2} \quad (1)$$

$$k_{on} = k_{+1} \quad (2)$$

$$k_{off} = k_{-1}k_{-2} / (k_{+2} + k_{-2}) \quad (3)$$

(a monophasic dissociation occurs if $k_{+2} \gg k_{-2}$, or if $(k_{+2} + k_{-2}) \gg k_{-1}$)

Figure 1. Detection of the complex between calmodulin and fluorescein-labelled peptides by native polyacrylamide gel electrophoresis. Complexes between calmodulin from bovine brain 1 μM; P2277, Sigma) and fluorescein-labelled skeletal MLCK-derived peptides ($\sim$1 μM) were prepared in gel buffer (25% gel mix (4 g sucrose + 1 mg bromophenol blue in water to give a 10 ml solution) + 75% TBSC (50 mM Tris-HCl, pH 7.4, 100 mM NaCl + 50 μM $CaCl_2$)) and run on a 15% native polyacrylamide gel (5 ml 30% acrylamide–bisacrylamide solution + 4.5 ml water + 0.5 ml 3 M Tris-base, pH 8.8, +1 μl 1 M $CaCl_2$ polymerised with 30 μl 25% ammonium persulphate and 9 μl TEMED) using 14.4 g/l glycine + 3 g/l Tris-base + 0.1 mM $CaCl_2$ as running buffer. In these conditions, the fluorescence of the positively charged labelled peptides can be detected on the gel only if they form a stable complex with calmodulin (Neri *et al*., 1995). No fluorescent band can be detected with non-correlated labelled peptides (data not shown). The gels were imaged with the luminescence analyser LUANA (Neri *et al*., 1996).

Peptides were made on a solid phase using a model 350 multiple peptide synthesizer (Zinsser Analytic, Frankfurt, Germany) employing Fmoc/*t*-butyl protecting groups. The Fmoc group was cleaved by 20% (v/v) piperidine in dimethylformamide and successive amino acids were added as *N*-hydroxybenzotriazole esters. The peptides were deprotected and cleaved from the resin by 93% trifluoroacetic acid, 3% 1,2-ethanedithiol, 2% anisole, 2% water. Peptides were analysed by high performance liquid chromatography using a Vydac C18 column (10 μM, 100 × 250 mm) and by amino acid analysis (PICO TAG, Waters, Milford, MA). The sequence of peptide 1 (wild-type) is shown, while 2 to 17 correspond to individual amino acid substitution to alanine. Peptides were labelled either with iodoacetamido fluorescein (Molecular Probes) or with iodoacetamido-LC-biotin (Pierce) essentially as described (Neri *et al*., 1995).

The number of the lane corresponds to the peptide number. The position of substitution is indicated with a line connecting the gel lane and the amino acid sequence (see also Table 1).

$$K_d = k_{off} / k_{on} \quad (4)$$

k_{isom} Constants have been measured by stopped-flow analysis, detecting changes in tryptophan fluorescence for all the peptides except 3, in which the tryptophan is replaced by alanine (Table 1). Measurements are made easy by the fact that calmodulin has no tryptophan residues. The stopped-flow kinetic profiles obtained are essentially monophasic over a time period of dozens of seconds, since the first association kinetic phase is essentially over after one second at the concentrations used. Figure 2(b) shows the experimental data for peptides 7 and 14, which display, respectively, the fastest and the slowest isomerisation rate. In general, k_{isom} values are not much affected by mutation to alanine; an exception is

made for 11 (N17 → A) and 14 (K20 → A), whose rates are one order of magnitude slower than that of the wild-type peptide 1.

We used real-time interaction analysis by surface plasmon resonance on a BIAcore instrument (Jönnsson *et al*., 1991) to determine k_{on} and k_{off} constants. We bound biotinylated peptides to streptavidin-coated microsensor chips, allowed calmodulin at different concentrations to associate with the peptides and monitored the association and dissociation of calmodulin as a function of time. The microsensor chip could be regenerated using Tris-buffered saline (TBS) + 15 mM EDTA, which dissociates the calmodulin–peptide complex. Figure 2(c) shows sensograms of peptides 1 and 5, in which the difference in k_{on} and k_{off} between the two peptides can be visually appreciated. It can also be noticed that the microsensor chip coated with peptide 1 is semi-saturated at approximately 5 nM calmodulin concentration, in good agreement with

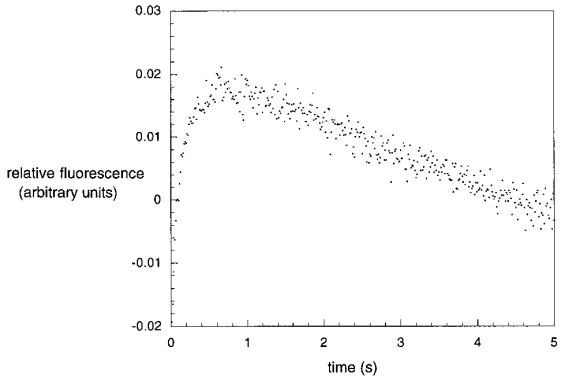

(a)

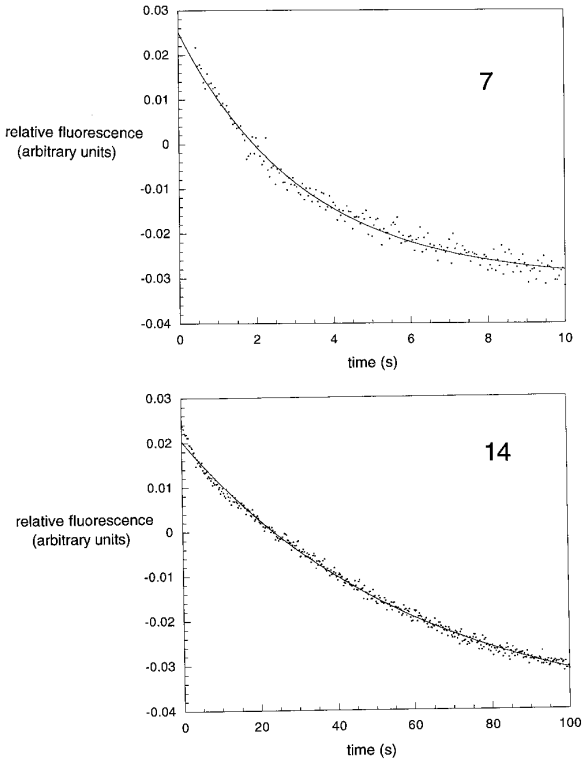

(b)

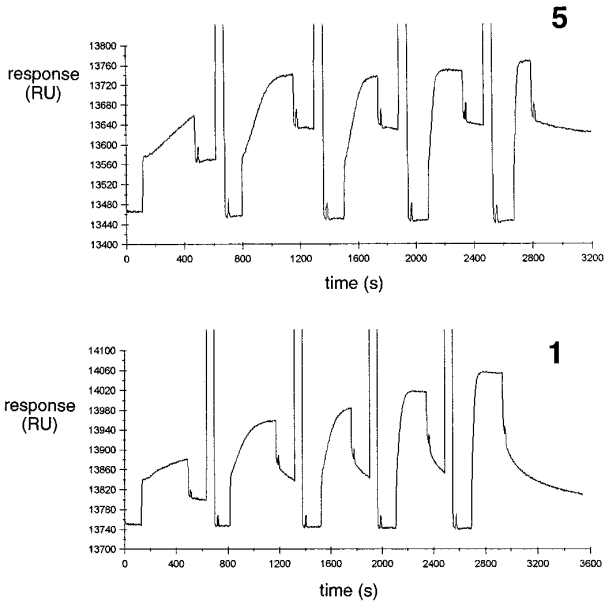

(c)

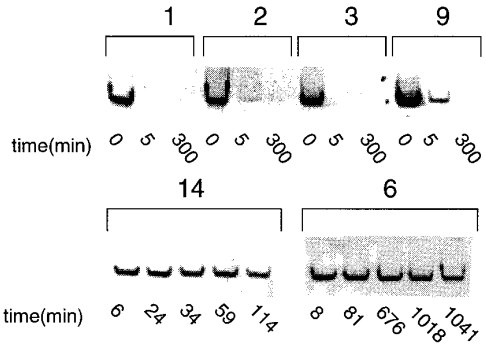

(d)

Figure 2(a–d) *legend on page 4*

Table 1. Kinetic analysis of the interaction between calmodulin and calmodulin-binding peptides by individual amino acid replacement to alanine

Peptide sequence:
0 1 2
1———————0———————0———
CAAA**RWKKNFI**A**VS**AA**NRFKKIS**

Pept.	Mutation	k_{isom} (s^{-1})[a]	k_{on} (s^{-1} M^{-1})[b]	k_{off} (s^{-1})[c]	k_{off} (s^{-1})[b]	K_d (M)[d]
1	wt	$1.9(\pm0.7) \times 10^{-1}$	$6.5(\pm1.6) \times 10^{5}$	$\geqslant 1 \times 10^{-3}$	$2.4(\pm0.6) \times 10^{-3}$	$3.7(\pm1.8) \times 10^{-9}$
2	R5 → A	$1.2(\pm0.5) \times 10^{-1}$	$3.0(\pm0.7) \times 10^{6}$	$\geqslant 1 \times 10^{-3}$	$1.5(\pm0.4) \times 10^{-3}$	$5.0(\pm2.5) \times 10^{-10}$
3	W6 → A	ND	$3.2(\pm0.8) \times 10^{6}$	$\geqslant 1 \times 10^{-3}$	$5.0(\pm1.2) \times 10^{-3}$	$1.6(\pm0.8) \times 10^{-9}$
4	K7 → A	$2.4(\pm0.6) \times 10^{-1}$	$1.3(\pm0.3) \times 10^{6}$	$\geqslant 1 \times 10^{-3}$	$3.0(\pm0.7) \times 10^{-3}$	$2.3(\pm1.1) \times 10^{-9}$
5	K8 → A	$7.4(\pm1.0) \times 10^{-2}$	$1.1(\pm0.3) \times 10^{6}$	$2.1(\pm1.0) \times 10^{-4}$	$2.9(\pm0.7) \times 10^{-4}$	$2.6(\pm1.3) \times 10^{-10}$
6	N9 → A	$1.8(\pm0.9) \times 10^{-1}$	$9.8(\pm2.5) \times 10^{5}$	$2.2(\pm1.1) \times 10^{-6}$	$<1 \times 10^{-4}$	$2.2(\pm1.4) \times 10^{-12}$
7	F10 → A	$2.5(\pm0.7) \times 10^{-1}$	$9.0(\pm2.2) \times 10^{5}$	$6.0(\pm3.0) \times 10^{-4}$	$3.9(\pm1.0) \times 10^{-4}$	$4.3(\pm2.1) \times 10^{-10}$
8	I11 → A	$1.1(\pm0.3) \times 10^{-1}$	$9.2(\pm2.3) \times 10^{5}$	$4.7(\pm2.3) \times 10^{-4}$	$2.3(\pm0.6) \times 10^{-4}$	$2.5(\pm1.2) \times 10^{-10}$
9	V13 → A	$1.5(\pm0.3) \times 10^{-1}$	$8.6(\pm2.1) \times 10^{5}$	$\geqslant 1 \times 10^{-3}$	$1.2(\pm0.3) \times 10^{-3}$	$1.4(\pm0.7) \times 10^{-9}$
10	S14 → A	$2.1(\pm1.0) \times 10^{-1}$	$1.1(\pm0.3) \times 10^{6}$	$7.9(\pm3.9) \times 10^{-5}$	$1.0(\pm0.2) \times 10^{-4}$	$9.1(\pm4.5) \times 10^{-11}$
11	N17 → A	$2.8(\pm0.6) \times 10^{-2}$	$9.4(\pm2.3) \times 10^{5}$	$4.9(\pm2.4) \times 10^{-4}$	$3.5(\pm0.9) \times 10^{-4}$	$3.7(\pm1.8) \times 10^{-10}$
12	R18 → A	$1.7(\pm0.4) \times 10^{-1}$	$1.6(\pm0.4) \times 10^{6}$	$8.3(\pm4.1) \times 10^{-4}$	$4.1(\pm1.0) \times 10^{-4}$	$1.8(\pm0.9) \times 10^{-10}$
13	F19 → A	$1.8(\pm0.8) \times 10^{-1}$	$9.3(\pm2.3) \times 10^{5}$	$\geqslant 1 \times 10^{-3}$	$8.4(\pm2.1) \times 10^{-4}$	$9.0(\pm4.5) \times 10^{-10}$
14	K20 → A	$1.6(\pm0.2) \times 10^{-2}$	$2.5(\pm0.6) \times 10^{6}$	$1.5(\pm0.7) \times 10^{-4}$	$1.4(\pm0.4) \times 10^{-4}$	$5.6(\pm2.8) \times 10^{-11}$
15	K21 → A	$1.2(\pm0.3) \times 10^{-1}$	$1.1(\pm0.3) \times 10^{6}$	$2.1(\pm1.0) \times 10^{-4}$	$2.2(\pm0.5) \times 10^{-4}$	$2.0(\pm1.0) \times 10^{-10}$
16	I22 → A	$8.7(\pm1.5) \times 10^{-2}$	$8.1(\pm2.0) \times 10^{5}$	$2.8(\pm1.4) \times 10^{-4}$	$3.1(\pm0.8) \times 10^{-4}$	$3.8(\pm1.9) \times 10^{-10}$
17	S23 → A	$1.3(\pm0.4) \times 10^{-1}$	$8.2(\pm2.0) \times 10^{5}$	$7.0(\pm3.5) \times 10^{-5}$	$1.3(\pm0.3) \times 10^{-4}$	$1.6(\pm0.8) \times 10^{-10}$

Bold face type indicates single-point mutations to alanine in individual peptides. ND, not determined.

[a] k_{isom} (s^{-1}) measured by stopped-flow as described in Figure 2.

[b] k_{on} (s^{-1} M^{-1}) and k_{off} (s^{-1}) measured by BIAcore as described in Figure 2. Only a condition is reported for k_{off} (s^{-1})[b] of peptide 6. This is due to the fact that measurement of very slow dissociation constants by BIAcore is made difficult by rebinding effects and by baseline instability, particularly when, like in the present study, calcium ions are used and the microsensor chip is derivatised to low surface density.

[c] k_{off} (s^{-1}) values measured by competition as described in Figure 2.

[d] K_d (M) = k_{off} (s^{-1})[b] / k_{on} (s^{-1} M^{-1})[b], except for peptide 6 for which K_d = k_{off} (s^{-1})[c] / k_{on} (s^{-1} M^{-1})[b].

the K_d value determined from k_{on} and k_{off}. The results of the BIAcore measurements are listed in Table 1.

In order to obtain an independent experimental confirmation of the BIAcore results, we determined constants by competition experiments, preforming calmodulin / fluorescein-labelled peptide complexes and incubating the resulting mixtures with the corresponding unlabelled peptides in molar excess for different times. The results of the competition were analysed by native polyacrylamide gel electrophoresis (Neri *et al*., 1995), using the cooled

Figure 2. Association and dissociation kinetics of calmodulin-binding peptides. (a) Relative fluorescence of peptide 12 (Table 1) upon binding to calmodulin as a function of reaction time. A record obtained by stopped-flow fluorimetry on rapid mixing of 8.3 μM calmodulin and 8.3 μM peptide 1 in TBSC (50 mM Tris-HCl, pH 7.4, 100 mM NaCl + 50 μM $CaCl_2$) is shown. Experiments were carried out at 25°C using an Applied Photophysics BioSequential DX-17MV. The relative fluorescence was monitored as a function of time with λ_{ex} = 280 nm and λ_{em} > 320 nm. The biphasic fluorescence change corresponds to a fast bimolecular association phase, followed by a slow isomerisation phase (Török & Trentham, 1994). (b) Isomerisation kinetics for peptides 7 and 14 detected by stopped flow. Conditions as in (a). Data points for the first 500 ms, corresponding to the fast kinetic association step (see (a)), are omitted from the plot and from the fitting procedure. The curves were fitted to a single exponential with a characteristic constant equal to k_{isom} (Table 1). (c) Typical sensograms of different concentrations of calmodulin binding to peptides 1 to 17, detected by real-time interaction analysis using a BIAcore instrument (5 μl / min flow rate; Jönsson *et al*., 1991) and TBSC buffer (50 mM Tris-HCl, pH 7.4, 100 mM NaCl + 50 μM $CaCl_2$). Here we show the results for peptides 1 and 5. Biotinylated peptides 1 to 17 (Figure 1) were bound to commercially available streptavidin-coated microsensor chips (Pharmacia Biosensor), in order to achieve a surface capacity of 100 to 200 resonance units (RU) of calmodulin bound. After each calmodulin injection (5, 10, 20, 50 and 100 nM in that order, see Figure), regeneration of the surface was achieved by injection of 5 μl TBS + 15 mM EDTA. k_{on} and k_{off} constants were obtained from the sensograms using the BIAevaluation software version 2.1, according to the manufacturer's instructions (Pharmacia Biosensor). (d) Competition experiments for the measurement of k_{off} constants for peptides 1 to 17 towards calmodulin. 30 nM fluorescein-labelled peptide / calmodulin complexes in gel buffer (Figure 1) were competed at room temperature for different times with 30-fold excess of unlabelled peptide. The resulting mixtures were run on native polyacrylamide gels and imaged by LUANA as described for Figure 1. The bands in the image obtained were integrated using the LUANA software (Neri *et al*., 1996) and the corresponding intensities plotted *versus* time and fitted with a single exponential, from which k_{off} constants were derived. In order to normalise bands intensities against pipetting errors, the samples contained 6 nM free fluorescein, which ran with the front. The fluorescein bands were integrated and used to normalise the calmodulin–fluorescent peptide complex band intensity. Here were show the results of the competitions for peptides 1, 2, 3, 6, 9 and 14. Incubation times (in minutes) are indicated under the lanes.

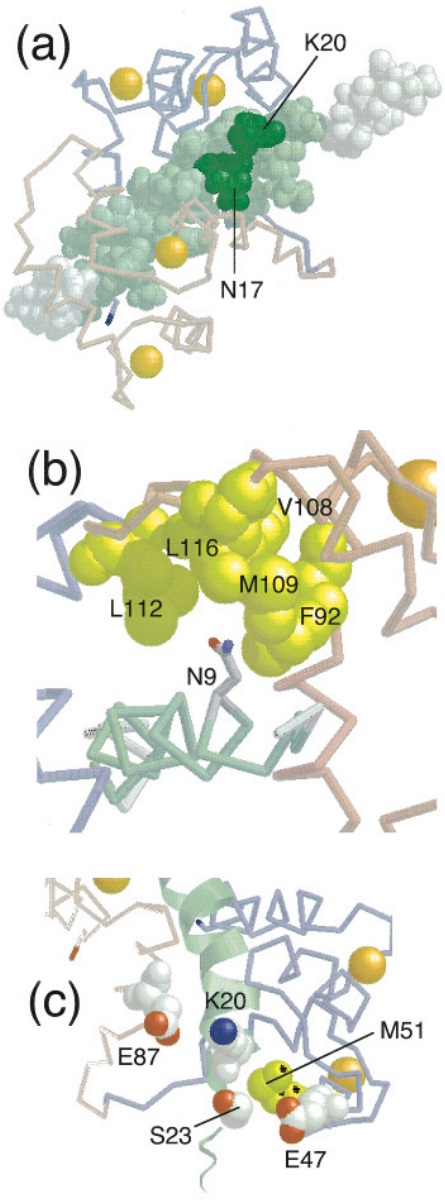

Figure 3. Structures of calmodulin in complex with skeletal MLCK-derived peptide. The NMR structure of the complex between calmodulin and skeletal MLCK-derived peptide (M13; Ikura *et al*., 1992), containing the RWKKNFIAVSAANRFKKIS recognition sequence (Figure 1; pale green), was used to analyse the effect of individual amino acid replacement to alanine on kinetics and thermodynamics of binding for the peptides listed in Table 1. The N-terminal domain of calmodulin is pale blue, the C-terminal domain pale red. Calcium atoms are orange. (a) Calmodulin wraps around the M13 peptide. Residues N17 and K20 (our numbering; Table 1), whose mutation to alanine slows down the isomerisation step depicted in Scheme 1, are drawn in dark green. (b) The side-chain of N9, whose substitution with alanine results in 1000-fold peptide affinity improvement towards calmodulin (Table 1), sits in a hydrophobic pocket defined by the side-chains of calmodulin F92, V108, M109, L112 ad L116 residues (yellow). (c) S23 (white; side-chain oxygen red) is the most C-terminal side-chain of M13 in contact with calmodulin. Its mutation to alanine may provide a hydrophobic interaction with M51 (yellow) and stabilise the interaction of K20 (white; side-chain nitrogen blue) with calmodulin E87 (white; side-chain oxygens red) and possibly E47 side-chains (white; side-chain oxygens red).

CCD-camera-based gel imager LUANA for high sensitivity detection and band integration (Neri *et al*., 1996). Figure 2(d) shows representative examples of the measurements. In the fast off-rate extreme, peptides 1, 2, 3 and 9 dissociate from calmodulin in a few minutes. Peptide 14 is representative of intermediate off-rate, whereas 6 is hardly competed by an excess of unlabelled peptide after 1000 minutes. The volumes of the bands were plotted *versus* competition time and fitted to a single exponential, from which k_{off} values were derived.

The fastest competitions (peptides 1 to 4, 9 and 13) were over by the time the calmodulin/fluorescent peptide complex entered the gel (approximately 5 to 10 minutes from pipetting a molar excess of unlabelled peptide; Figure 2(d)), from which a condition on the off-rate constant $k_{off} \geqslant 1 \times 10^{-3}\ s^{-1}$ was derived. Even for these fast off-rates, complexes can be detected by native polyacrylamide gel electrophoresis because of the well-known gel ''cage effect'' (Fried & Crothers, 1981; Garner & Revzin, 1981). The k_{off} values measured by competition and by BIAcore are in substantial agreement (Table 1). Small differences between the two sets of data may be due to the fact that competition experiments were performed in gel mix buffer (Figure 2(d)) rather than in TBS + 50 μM $CaCl_2$. The monophasic dissociation observed in both BIAcore and competition experiments confirms the assumption of equation (3).

The results summarised in Table 1 have the following implications.

(1) The k_{isom} values of the peptides examined are similar, except for 11 (N17 → A) and 14 (K20 → A), which show a tenfold slower isomerisation rate. Figure 3(a) shows how the two mutations map to peptidic side-chains in close spatial proximity. The concerted interaction of peptidic N17 and K20 (separated by one helix turn) with the negatively charged E84 and E87 in calmodulin (Ikura *et al*., 1992) is therefore probably important for speeding up the isomerisation from P–C to P–C* (Scheme 1). NMR spectroscopy (Wüthrich, 1986) may be a suitable technique for investigating the isomerisation mechanism at a molecular level (Erhardt *et al*., 1995).

(2) Kinetic association constants k_{on} of skeletal MLCK-derived peptides 1 to 17 are in the range 6.5×10^5 to $3.2 \times 10^6\ s^{-1}\ M^{-1}$, and are more than 100-fold lower than those of smooth muscle MLCK-derived peptides (Török & Trentham, 1984). The largest increase in k_{on} with respect to the wild-type peptide 1 was observed for R5, W6 and K20 mutations to alanine (4 to 5-fold increase; Table 1). Thus alanine mutations of two positively charged amino acid residues (R5 and K20) are associated with increased on-rates. Changes in k_{on}

are smaller for mutations involving hydrophobic side-chains (Table 1).

(3) Alanine mutations can improve k_{off} values up to 1000-fold with respect to the wild-type peptide 1 (Table 1). The largest improvements are observed for hydrophilic residues (N9, S14, S23), which are not stable in the hydrophobic environment of the calmodulin core. The side-chain of N9 sits in a hydrophobic pocket surrounded by residues F92, V108, M109, L112 and L116 of calmodulin (Ikura *et al*., 1992; Afshar *et al*., 1994; and Figure 3(b)). It will be interesting to test whether this observation on the stability of asparagine side-chains in hydrophobic pockets without being engaged in hydrogen bonding has more general validity. On the contrary, buried asparagine residues in bovine pancreatic trypsin inhibitor (BPTI) involved in hydrogen bonding are associated with a higher thermal stability than the corresponding alanine mutants (Yu *et al*., 1995). Work is in progress to ascertain whether N9 substitutions to hydrophobic residues other than alanine result in even greater improvements in affinity.

S23 is partly water exposed, but its mutation to alanine may result in a favourable interaction with M51 and help to stabilise the interaction of K20 with calmodulin E47 and E87 side-chains (Figure 3(c)). One may speculate whether the helix-stabilising properties of alanine (Horovitz *et al*., 1992) contribute to the improvements in K_d and k_{off} values reported in Table 1. The helix stabilisation for alanine mutations of solvent exposed serine, arginine and lysine residues are negligible ($\Delta\Delta G_\alpha \leqslant 0.5$ kcal/mol) and no stabilisation greater than 1 kcal/mol is expected for the residues mutated in our peptides (Horovitz *et al*., 1992). It is possible that these stabilisation energies may increase in a hydrophobic milieu such as the hydrophobic core of calmodulin, but it would be difficult to separate helix stabilisation effects from specific side-chain interactions with calmodulin. Fersht *et al*. (1985) described a serine-to-alanine mutation in a hydrophobic cavity of tyrosyl-tRNA synthetase that increased by tenfold the enzyme affinity for its substrate. However, the lesson learned from protein stability studies shows that mutations of buried serine residues can be stabilising or destabilising, depending on the macromolecular environment (see, for example, Blaber *et al*., 1995; Yu *et al*., 1995). When mutating serine residues, the hydroxyl group of serine can be replaced by a water molecule (Blaber *et al*., 1995; Berndt *et al*., 1993), which may be engaged in hydrogen bonding and may influence the energetics of the macromolecule under investigation.

Our observations are consistent with that of Török & Trentham (1994), who noticed that the Ac–RRK-WQKTGHAVRAIGRL–$CONH_2$ smooth muscle MLCK-derived peptide has 1000-fold higher affinity than the homologue RRKWQKTGHAVR-AIGRLSSS–$CONH_2$ containing three additional buried C-terminal serines.

(4) The increases in affinity caused by single-point mutations to alanine in peptide 1 (K_d values in Table 1) contradict certain theoretical predictions. Afshar *et al*. (1994) postulated a ''dominant role of the electrostatic force for high-affinity interaction'', with particular reference to positions K8 and R18 (our numbering), for each of which they calculated an interaction energy with calmodulin of approximately –100 kcal/mol (for comparison's sake, note that the total $\Delta G^{binding}$ for the subpicomolar RNase inhibitor barstar at neutral pH and at 25°C amounts to about –20 kcal/mol; Schreiber *et al*., 1994). Our data show that mutations of K8 and K18 to alanine increase the affinity of the peptide towards calmodulin by more than tenfold.

W6 and F19 were also postulated to be important for binding, with a calculated interaction energy to calmodulin of more than –10 kcal/mol. However, these positions can be mutated to alanine without loss of calmodulin binding affinity. Even if the interaction energies calculated by Afshar *et al*. (1994) are correct, it is difficult to use those values to make predictions about affinities. The energy of binding of two proteins is, in fact, the difference between the energy of the two components in the bound state and the energies of the same components in aqueous solutions.

(5) Calmodulin binding to skeletal myosin light chain kinase seems to have evolved to perform its biological function by achieving sufficiently high affinity, but far from the maximum. On the basis of the data presented in Table 1 and the data for smooth muscle MLCK (Török & Trentham, 1994), one wonders whether these enzymes have evolved to have off-rates that allow them to dissociate from calmodulin after activation. Calmodulin binding of kinases and calmodulin-binding peptides can be abolished by casein kinase II-mediated phosphorylation (Quadroni *et al*., 1994; D.N., unpublished results). Our data confirm that the isomerisation step observed for calmodulin modified with a fluorescent probe occurs also in unmodified calmodulin upon substrate binding. It will be interesting to measure the dependence of k_{isom} on Ca^{2+} concentration, in particular at physiological Ca^{2+} levels, and to investigate as suggested by Török & Trentham (1994), whether the isomerisation step is physiologically significant.

(6) The calmodulin–peptide complex system has the unique property of coupling very high binding affinity (even in the presence of detergents, D.N. & R. Grisshammer, unpublished results) with mild release conditions by addition of calcium chelators. This is attractive for biotechnological applications (Neri *et al*., 1995); for protein purification and detection, conditional formation of bifunctional (macro)molecules, microscopy, FACS analysis, protein immobilisation on microsensor chips and tumour targeting. For many of these applications, it is desirable to have very high affinities, with fast on-rates and slow off-rates. Peptide 6 meets some of these characteristics (Table 1). Smooth muscle MLCK-derived peptides bind to calmodulin with

$k_{on} > 10^8$ l/sM but relatively poor k_{off} (Török & Trentham, 1994). Applications such as *in vivo* tumour targeting (Paganelli *et al*., 1991) may benefit from improving the k_{off} of smooth muscle MLCK-derived peptides; for example, by alanine-scanning investigation and stringent selection of designed peptide libraries displayed on filamentous phage (Scott, 1992).

One of the problems for the use of calmodulin binding peptides as useful protein tags (Stofko-Hahn *et al*., 1992) is their susceptibility to proteolysis at the level of adjacent basic residues in bacterial secretion systems (Neri *et al*., 1995). The data presented in Table 1 suggest that dibasic sequences in calmodulin-binding peptides may be mutated without loss (and even with gain) in affinity. This may represent one of the relevant parameters for a designed peptide library on phage, to be selected for both calmodulin binding and resistance to proteolysis.

(7) Individual replacements of contact residues with alanine in macromolecular complexes of known three-dimensional structure have resulted in affinity loss and so allowed the identification of the specified residues important for binding (e.g. see Clackson & Wells, 1995; Schreiber *et al*., 1994). In this respect the results in Table 1, in which no amino acid residue appears to be essential for binding, are counter-intuitive. However, while the proteins in the reference cited interact with a relatively flat surface, peptides are completely wrapped by calmodulin. The different lesson learned from alanine scanning experiments with calmodulin-binding peptides may reflect this different mode of binding.

Alanine scanning of calmodulin binding peptides does not highlight residues that individually account for a large part of the binding energy (see Bigler *et al*., 1993, for interesting discussion on isofunctional residues). This does not exclude, however, a ''reductionist'' approach and indeed small synthetic inhibitory molecules for calmodulin have been found. For example, the small indole derivative melatonin binds to calmodulin with K_d = 188 pM (Benitez-King *et al*., 1993). W6 → A does not reduce the peptide's affinity for calmodulin. The cleft that accommodates the indole ring of W6 is well visible in the C-terminal domain of the calmodulin structure (Ikura *et al*., 1992). A structure-based approach that identifies clefts in a protein surface may therefore be a sufficient starting point for a structure-based design of a good inhibitor.

It will be interesting to investigate the extent to which the affinity improvements arising from these single alanine mutations are additive. While additivity was demonstrated for the binding of human growth hormone mutants to its receptor (Lowman & Wells, 1993), calmodulin binding peptides may reserve a few surprises for us, especially if combined mutations do not add up linearly in terms of solvation energy of the peptides due to intramolecular interactions in the unbound state.

References

Afshar, M., Caves, L. S. D., Guimard, L., Hubbard, R. E., Calas, B., Grassy, G. & Haieck, J. (1994). Investigating the high affinity and low sequence specificity of calmodulin binding to its targets. *J. Mol. Biol.* **244**, 554–571.

Bayer, E. A. & Wilchek, M. (1990). Protein biotinylation. *Methods Enzymol.* **184**, 138–160.

Benitez-King, G., Huerto-Delgadillo, L. & Anton-Tay, F. (1993). Binding of ^{3}H-melatonin to calmodulin. *Life Sci.* **53**, 201–207.

Berndt, K. D., Beunink, J., Schroder, W. & Wüthrich, K. (1993). Designed replacement of an internal hydration water molecule in BPTI: structural and functional implications of a glycine-to-serine mutation. *Biochemistry*, **32**, 4564–4570.

Bigler, T. L., Lu, W., Park, S. J., Tashiro, M., Wieczorek, M., Wunn, R. & Laskowski, M. Jr. (1993). Binding of amino acid side-chains to preformed cavities: interaction of serine proteinases with turkey ovomucoid third domains with coded and noncoded P1 residues. *Protein Sci.* **2**, 786–799.

Blaber, M., Baase, W. A., Gassner, N. & Matthews, B. W. (1995). Alanine scanning mutagenesis of the α-helix 115–123 of phage T4 lysozyme: effects on structure, stability and the binding of solvent. *J. Mol. Biol.* **246**, 317–330.

Clackson, T. & Wells, J. A. (1995). A hot-spot of binding energy in a hormone–receptor interface. *Science*, **267**, 383–386.

Erhardt, M. R., Urbauer, J. L. & Wand, A. J. (1995). The energetics and dynamics of molecular recognition by calmodulin. *Biochemistry*, **34**, 2731–2738.

Fersht, A. R., Wilkinson, A. J., Carter, P. & Winter, G. (1985). Fine structure–activity analysis of mutations at positions 51 of tyrosyl-tRNA synthetase. *Biochemistry*, **24**, 5858–5861.

Fried, M. & Crothers, D. M. (1981). Equilibria and kinetics of lac repressor-operator interactions by polyacrylamide gel electrophoresis. *Nucl. Acids Res.* **9**, 6505–6525.

Garner, M. M. & Revzin, A. (1981). A gel electrophoresis method for quantifying the binding of proteins to specific DNA regions: applications to components of the *Escherichia coli* lactose operon regulatory system. *Nucl. Acids Res.* **9**, 3047–3060.

Horovitz, A., Matthews, J. M. & Fersht, A. (1992). α-Helix stability in proteins. II. Factors that influence stability at internal position. *J. Mol. Biol.* **227**, 560–568.

Ikura, M., Clore, G. M., Gronenborn, A. M., Zhu, G., Klee, C. B. & Bax, A. (1992). Solution structure of a calmodulin-target peptide complex by multidimensional NMR. *Science*, **256**, 632–638.

Jönsson, U., Fägerstam, L., Ivarsson, B., Johnsson, B., Karlsson, R., Lundh, K., Löfås, S., Persson, B., Roos, H., Rönnberg, I., Sjölander, S., Stenberg, E., Ståhlberg, Urbaniczky, C., Östlin, H. & Malmqvist, M. (1991). Real-time biospecific interaction analysis using surface plasmon resonance and a sensor chip technology. *BioTechniques*, **11**, 620–627.

Lowman, H. B. & Wells, J. A. (1993). Affinity maturation of human growth hormone by monovalent phage display. *J. Mol. Biol.* **234**, 564–578.

Lukas, T., Haiech, J., Lau, W., Craig, T. A., Zimmer, W. E., Shattuck, R. L., Shoemaker, M. O. & Watterson, D. M. (1988). Calmodulin and calmodulin-regulated protein kinases as transducers of intracellular calcium

signals. *Cold Spring Harbor Symp. Quant. Biol.* **53**, 185–193.

Meador, W., Means, A. & Quiocho, F. (1992). Target enzyme recognition by calmodulin: 2.4 Å structure of a calmodulin–peptide complex. *Science*, **257**, 1251–1257.

Meador, W., Means, A. & Quiocho, F. (1993). Modulation of calmodulin plasticity in molecular recognition on the basis of X-ray structures. *Science*, **262**, 1718–1721.

Neri, D., de Lalla, C., Petrul, H., Neri, P. & Winter, G. (1995). Calmodulin as a versatile tag for antibody fragments. *Bio/Technology*, **13**, 373–377.

Neri, D., Prospero, T., Petrul, H., Winter, G., Browne, M. & Vanderpant, L. (1996). A multi-purpose high sensitivity luminescence analyser (LUANA): use in gel-electrophoresis. *BioTechniques*, in the press.

O'Neil, K. & DeGrado, W. (1989) The interaction of calmodulin with fluorescent and photoreactive model peptides: evidence for short interdomain separation. *Proteins: Struct. Funct. Genet.* **6**, 284–293.

Paganelli, G., Magnani, P., Zito, F., Villa, E., Sudati, F., Lopalco, L., Rossetti, C., Malcovati, M., Chiolerio, F., Seccamani, E., Siccardi, A. G. & Fazio, F. (1991 Three-step monoclonal antibody tumour targeting in carcinoembryonic antigen-positive patients. *Cancer Res.* **51**, 5960–5966.

Quadroni, M., James, P. & Carafoli, E. (1994). Isolation of phosphorylated calmodulin from rat liver and identification of the in vivo phosphorylation sites. *J. Biol. Chem.* **269**, 16116–16122.

Schreiber, G., Buckle, A. M. & Fersht, A. (1994). Stability and function: two constraints in the evolution of barstar and other proteins. *Structure*, **2**, 945–951.

Scott, J. K. (1992). Discovering peptide ligands using epitope libraries. *Trends Biochem. Sci.* **17**, 241–245.

Stofko-Hahn, R. E., Carr, D. W. & Scott, J. D. (1992). A single step purification for recombinant proteins. *FEBS Letters*, **302**, 274–278.

Török, K. & Trentham (1994). Mechanism of 2-Chloro-(ϵ-amino-Lys75-[6-4-(*N*,*N*-diethylamino)phenyl]-1,3,5-triazin-4-yl) calmodulin interactions with smooth muscle myosin light chain kinase and derived peptides. *Biochemistry*, **33**, 12807–12830.

Wüthrich, K. (1986). *NMR of Proteins and Nucleic Acids*, Wiley, New York.

Yu, M. H, Weissman, J. S. & Kim, P. S. (1995). Contribution of individual side-chains to the stability of BPTI examined by alanine-scanning mutagenesis. *J. Mol. Biol.* **249**, 388–397.

Edited by F. Cohen

(Received 10 November 1995; received in revised form 7 February 1996; accepted 8 February 1996)